for lower carbon contents, which may be real and point toward an additional effect. A decision whether the resistivity increase with decreasing carbon content is solely due to increased vacancy scattering cannot be made at present.

ACKNOWLEDGMENTS

The work of a large number of co-workers is acknowledged with thanks. N. Mady prepared most of the samples, fabricated the TaC crucibles, and performed the resistivity measurements. J. Gitto cooperated in many phases of the experimental work. Dr. H. Juretschke of the Polytechnic Institute of Brooklyn made the measurements of the magnetic susceptibility.

Thanks are especially due to Dr. L. L. Seigle, under whose direction this work was performed, for many valuable discussions.

JOURNAL OF APPLIED PHYSICS VOLUME 37, NUMBER 9 AUGUST 1966

Penetration Parameter for an Adsorbed Layer of Polarizable Ions

J. Ross Macdonald and C. A. Barlow, Jr.
Texas Instruments Incorporated, Dallas, Texas
(Received 27 September 1965; in final form 14 March 1966)

We present several improvements in the calculation of the penetration parameter f, which is related to ionic and electronic work functions. A regular, hexagonal array of adions which are imaged in a conducting adsorbent plane is considered. The first improvement is the treatment of discrete adion charges and their images as non-ideal, finite-length dipoles instead of ideal dipoles as in almost all earlier treatments. Next, nonzero polarizability of adions is considered, discrete induced dipole moments are calculated in a self-consistent manner, and the effect of induced-dipole images is included. When the polarizability is nonzero, previous expressions for f are inadequate even when generalized in an obvious way, and an improved method of calculating f is presented. The inclusion of polarization effects leads to significant changes in the dependence of f on surface coverage of adions. Finally, f is calculated with and without polarization contributions for the situation where redistribution of the adsorbed array upon removal of an adion affects the desorption energy. Inclusion of redistribution also leads to appreciable changes in f. Under some circumstances, either with or without redistribution contributions, it is found to be easier to desorb an adion from an array than to desorb an isolated adion. In this case, the potential at the site of a removed adion may exceed that far away from the surface. To illustrate this phenomenon, which can lead to the establishment of a potential barrier against electron emission, or to a potential well enhancing emission, we give some curves of potential vs distance from the electrode along a line perpendicular to the electrode and through a removed adion site.

INTRODUCTION

CONSIDER an infinite two-dimensional array of ions absorbed on an electrically conducting plane surface. The adion charges will be imaged in the absorbent, forming an array of non-ideal dipoles. The array penetration parameter f, which in its most basic definition is essentially the ratio of the change of ionic to the change of electronic work function upon adsorption, is of considerable importance in the adsorption of ions from a gas phase, and it or its equivalent has appeared in a number of treatments of the adsorption of cesium on tungsten and thermionic energy conversion.[1–6]

In theoretical treatments of the penetration parameter, several different definitions and ways of calculating f have been introduced which, though generally assumed to be equivalent to the foregoing definition, unfortunately turn out to be nonequivalent to this definition and to each other for finite adion polarizability α, interaction with self-images, and the occurrence of adion redistribution effects. While certain of these definitions have no physical significance except to the degree that they approximate to the actual quantity sought, others possess a direct physical interpretation and, though not representing the "true penetration parameter" as originally defined, are of sufficient interest in themselves to warrant some discussion. Finally, whereas there is one definition which is admittedly no more than an approximation to the measured f, the situation is not so clearcut as regards the other definitions: In certain cases, one manner of theoretically calculating f may be proper, and in other cases the circumstances may have altered enough to make another method appropriate. It is the purpose of this paper to clarify for the first time this situation by discussing and comparing several

[1] J. H. de Boer, Advan. Catalysis 8, 119 (1956).
[2] N. S. Rasor, C. Warner, II, and A. R. Vernon, Atomics International Report No. AI-6799 (November 1961), pp. 51–55, 81–109; C. Warner, II, and L. K. Hansen, Atomics International Report No. AI-64-20 (November 1962–October 1963), pp. 110–140.
[3] A. J. Kennedy, Advan. Energy Conversion 3, 207 (1963).
[4] J. W. Gadzuk, MIT Quart. Progr. Rept. No. 72 (15 January 1964), pp. 166–171; No. 75 (15 October 1964), pp. 104–106.
[5] N. S. Rasor and C. Warner, J. Appl. Phys. 35, 2589 (1964).
[6] J. W. Gadzuk and E. N. Carabateas, J. Appl. Phys. 36, 357 (1965).

different theoretical objects, distinguishing them from the "true f" by means of the humble, subscripted names: f_1, f_2, and so forth. While we recognize that our subscripted quantities may not end up being entirely equivalent to the measured f, we shall nonetheless refer to these theoretical constructs as "definitions of f." Three different expressions for f are given below and each is discussed in some detail for the general case $\alpha \neq 0$ later in the paper.

All published theoretical calculations of f thus far have neglected adion redistribution effects and, except for Ref. 5 (an oversimplified approach), have treated the effective dipoles as ideal and the ions as nonpolarizable. We have recently developed a practical method for calculating the field and potential exactly anywhere in front of an infinite plane conducting surface on which an infinite regular array of nonpolarizable ions are absorbed and imaged.[7] In the present paper, which uses and extends this work, we wish to compare the results for f for real, polarizable, non-ideal dipoles with those of previous calculations and methods.

At absolute zero an adsorbed array of ions may be considered rigid (except for minor vibrations arising from the zero-point energy of the adions). As the temperature increases, the amplitude of the vibrations increases until finally, although the adions may still remain strongly adsorbed, their position correlations extend only over short distances and the concept of a regular array is no longer applicable. We have established approximate conditions for which a regular rather than completely disordered array is a good model,[8] and Vernon[2] has given preliminary consideration to the direct effect on f of thermal disordering. His approach has been somewhat extended by Gadzuk and Carabateas.[6]

Since the effects of thermal motion may be considered as perturbations to a regular array within the regime where the two-dimensional discrete charge distribution still retains appreciable long-range ordering, the influence of thermal disordering within this range will be a perturbation to the fixed-array value of f. The effect of this perturbation may be calculated separately by a variety of techniques; thus, it is important to have a reasonably accurate expression for f for a regular array as the start of a calculation of f in the presence of some thermal disorder. Such a calculation is in progress; here we are solely concerned with regular arrays and we ignore any vibration of the adions. This approximation is still a good one for many conditions of experimental interest.[8]

Since the surface of a metal is not a featureless continuum but a two-dimensional array of atoms, there will be potential wells or preferred sites on it for the adsorption of foreign atoms or ions. In equilibrium at zero degrees, all adions will be localized at such sites. On the other hand, at nonzero temperatures where adions have translational energy they may hop between sites.[9] At still higher temperatures where the adions are still strongly constrained to the surface by "chemical" and image forces, the influence of preferred sites becomes small and the adions are no longer strongly localized but can move relatively freely along the adsorbent surface. This last condition may still be one, however, where the mutual repulsion of the non-ideal dipoles formed by the adions imposes appreciable long-range order on the array. In this mobile case, the array will tend to be hexagonal since this configuration maximizes r_1, the nearest-neighbor spacing, for a given surface density N. Further, if the ions could be close-packed on the surface, the array would again be hexagonal. In neither of these cases would r_1 be determined by the number of preferred sites but instead $r_1 = (\frac{4}{3})^{\frac{1}{2}} N^{-\frac{1}{2}}$. Note that we can write $N \equiv \theta N_s$, where N_s is the maximum surface density possible in a monolayer[7,10] and $0 \leq \theta \leq 1$.

The usual localized film model is one in which a fraction θ of N_s regularly arranged sites is occupied.[7] Excellent reasons for not calling this an immobile film have been advanced by Holland[9] and by Ross and Olivier.[11] We shall here be primarily concerned with mobile adions and shall not consider this localized model in further detail except to mention that when $\alpha = 0$ the f appropriate to it can easily be derived from that of the mobile model by a procedure discussed later.

Gadzuk and Carabateas[6] have introduced an uncommon definition for an immobile array. They consider a cubic adsorbent with lattice constant d. A fixed, square array is assumed to be present having a minimum r_1 of $2d$ when $\theta = 1$. A complete, regular square array is also assumed to be present under other conditions, but only values of θ are allowed which are associated with r_1 values of $2dn$, where $n = 1, 2, 3 \cdots$. For square arrays, r_1 is then equal to $2d/(\theta_n)^{\frac{1}{2}}$; thus, $\theta_n \equiv n^{-2}$. Except for the difference between square and hexagonal arrays, the model is equivalent to the mobile model for the above possible values of θ. Note, however, that Gadzuk and Carabateas ignore the discreteness in θ values occasioned by their model in plotting a curve of $f(\theta_n)$. We shall later transform these square-array results to a hexagonal basis for comparison with the hexagonal, mobile model. The latter has also been used by Kennedy[3] for adsorption of cesium on refractory metals. Gadzuk and Carabateas have also introduced an unusual definition for mobile films. Their definition is equivalent to that we have termed localized films,

[7] C. A. Barlow, Jr., and J. R. Macdonald, J. Chem. Phys. **43**, 2575 (1965).

[8] J. R. Macdonald and C. A. Barlow, Jr., Can. J. Chem. **43**, 2985 (1965).

[9] B. W. Holland, Trans. Faraday Soc. **61**, 546 (1965).

[10] J. R. Macdonald and C. A. Barlow, Jr., J. Chem. Phys. **39**, 412 (1963); **40**, 237 (1964). An important correction to some of this work is discussed in the present Ref. 13.

[11] S. Ross and J. P. Olivier, *On Physical Adsorption* (Interscience Publishers, Inc., New York, 1964), pp. 13–15.

types of films which have frequently been designated as immobile in the past.[10,12]

In the present work, it is assumed that when the adions are not close-packed there is no extraneous polarizable material between them. If they had no polarizability and were thus true monopoles, the dielectric constant appearing in potential and field calculations would be unity. Although the polarizability of adions is much smaller than that of adatoms, it is still nonzero and cannot always be neglected.[10,13] The depolarizing field of surrounding adions and their images will induce an essentially ideal dipole in any given polarizable adion. This dipole will then itself be imaged in the adsorbent surface causing an increase in effective adion polarizability and induced dipole moment.[10,13] Gadzuk and Carabateas have omitted all polarizability effects from their calculation of f on the basis that an approximate calculation with $\alpha \neq 0$ leads to little alteration in f values. By using the results of a much less approximate calculation, we shall show that this is not always the case.

DEFINITIONS OF f

Let us define the mean ionic charge density corresponding to N adions per unit area as q_a. We shall take the conducting adsorbent plane to be grounded; its charge density q will then be just $-q_a$. It will be convenient to take the zero of potential at the electrode and define ψ_∞ as the potential, arising from the adion-image array, at an "infinite" perpendicular distance from the adsorbing plane. For a plane array of infinite extent, the distance to "infinity" is any distance large compared to r_1. When the array is of finite size, the point at "infinity" must also be taken at a distance from the surface small compared with the smallest linear dimension of the lattice. Note that ψ_∞ is relatively independent of array structure[10,13]; it will be independent when $\alpha = 0$ and when the array, even though thermally disordered, is uniform in the large so q_a is independent of locale. Let ΔW_e be the average electron work function change on adion adsorption.[10] Then ΔW_e may be defined as the energy to remove to "infinity" an electron from the surface in the presence of an adsorbed array minus that required when no array is present. Since the work function of the bare surface is not included in ψ_∞, $\Delta W_e \equiv -e\psi_\infty$.

In analogy to the above, let ΔW_i be the change in ionic work function on adion desorption. It is the energy required to remove an adion from its equilibrium position in the array to "infinity" minus that required in the limit $N \to 0$, when the ion to be removed has no neighbors. By definition then, we may write $f \equiv -\Delta W_i / z_v \Delta W_e$, independent of the sign of z_v, the adion effective valence. Note that since an adion will generally be bound chemically as well as electrically to the adsorbent surface, W_i should properly include a contribution from such binding. To a good approximation, such binding should be independent of N, however, at least until surface packing is very dense. With such independence, chemical binding contributions will cancel when the difference ΔW_i is formed, and we thus ignore them hereafter.

The energy of ionic adsorption will generally include a part arising from redistribution of the regular array to make room for an added adion. After adsorption and redistribution, the array of mobile adions will still be regular, but its r_1 will be very slightly smaller. Inclusion of the redistribution energy in the adsorption or desorption energy is not always warranted, however. The ionic desorption energy W_i should include the redistribution contribution provided desorption is quasistatic or takes place in a time long compared to the array redistribution time. Although the average r_1 will be infinitesimally changed by desorption of a single adion, the nearest neighbors of this adion must move during redistribution a distance of about $r_1/2$. In many cases of interest, they will approach their new equilibrium positions before the desorbed ion has left the immediate vicinity of the surface. Under such circumstances, the ionic work function should include the redistribution energy contribution. We therefore include it in one of our calculations of f. For completeness, we shall also consider the case where the ion is removed from electrical interaction with the surface in so short a time that redistribution has not taken place and its contribution can be omitted from the desorption work. Further, in the case of localized adsorption, redistribution will be impeded by the potential wells which localize adions and, depending on the depth of the wells and the consequent strength of localization, little or no redistribution may occur during the time of removal of an adion on desorption from such an array.

Let us initially ignore redistribution energy and consider the simplest, most usual, but least accurate expression for f. Let z be the distance coordinate perpendicular to the adsorption plane and define β as the perpendicular distance from the imaging plane of the adsorbent to the charge centroid position of an adion. Contributions to β have been discussed elsewhere[7,10,14]; it will be approximately equal to the hard-core radius of the adion. With the adion itself removed completely, together with the images of its charge and induced dipole, define the potential at the position of the missing adion (point a) as ψ_a. This potential, which applies at the distance β in front of the surface, arises solely from all surrounding regularly arranged adions and their images. Thus, $(\psi_\infty - \psi_a)$ is the potential difference associated with

[12] A. R. Miller, Proc. Cambridge Phil. Soc. 42, 292 (1946); *The Adsorption of Gases on Solids* (Cambridge University Press, Cambridge, England, 1949), pp. 112–113.

[13] J. R. Macdonald and C. A. Barlow, Jr., J. Chem. Phys. 44, 202 (1966). The quantity p in this work is not the same as the p of the present paper and that of Ref. 18.

[14] J. R. Macdonald and C. A. Barlow, Jr., J. Chem. Phys. 36, 3026 (1962).

removing an adion from its equilibrium position in a complete lattice to "infinity," omitting redistribution, chemical effects, and contributions arising from the ion's own images. Within these approximations, $\Delta W_i = z_v e(\psi_\infty - \psi_a)$ and f becomes[2,4-6]

$$f_1 \equiv 1 - [\psi_a/\psi_\infty]. \tag{1}$$

As we shall see later, the contribution from the removed adion's own charge image and chemical binding effects properly do not appear in Eq. (1). Since the induced dipole moment of an adion depends upon N, however, the effect of the image of this dipole will not cancel in the later more accurate definitions of f, and its influence should be included. Let us designate quantities pertinent when $\alpha \equiv 0$ with a superscript zero; then, $f_1^0 = 1 - [\psi_a^0/\psi_\infty^0]$. Even this simplified quantity has not been calculated accurately heretofore except in our own recent work[7] because of the usual replacement of the array of non-ideal dipoles formed by the adion charges and their images by an ideal dipole array or other type of approximation.

In order to develop the next definition of f, denote the potentials at point a (missing-adion site) arising from the images of the adion charge and its induced dipole as ϕ_m and ϕ_d, respectively. These potentials are evaluated as though the adion were in its equilibrium position; thus, the images appear to be a distance of 2β from point a. Let $\phi_i \equiv \phi_m + \phi_d$ and $\psi_i \equiv \psi_a + \phi_i$. Then, one might expect that an expression for ΔW_i superior to that given above would be $\Delta W_i = z_v e[(\psi_\infty - \psi_i)_N - (\psi_\infty - \psi_i)_0] \equiv z_v e[\psi_\infty - \Delta\psi_i]$, since ψ_∞ is zero for $N = 0$. This expression counts self-image energy terms at their full value, but since they arise from self-images only half of each full contribution is appropriate. Thus, let $\psi_e \equiv \psi_i - (\phi_i/2) = \psi_a + (\phi_i/2)$. A detailed and relatively complicated consideration of individual ionic work function energy terms shows that in the absence of redistribution, as one might expect, $\Delta W_i = z_v e[\psi_\infty - \Delta\psi_e]$; thus let us define

$$f_2 \equiv 1 - [\Delta\psi_e/\psi_\infty], \tag{2}$$

where

$$\Delta\psi_e = \psi_a + \tfrac{1}{2}[\phi_d - \phi_{d0}]. \tag{3}$$

Here ϕ_{d0} is the value of ϕ_d at $N = 0$; the value of ψ_a in this limit is zero; and chemical and image charge terms have cancelled out of $\Delta\psi_e$. Suppose we now define the following function of r_1:

$$T \equiv -[\phi_d - \phi_{d0}]/2\psi_\infty. \tag{4}$$

Then, Eqs. (1)–(4) yield

$$f_2 = f_1 + T, \tag{2a}$$

showing how the more accurate f_2 differs from f_1. Note, however, that $f_2^0 = f_1^0$.

In order to obtain the f appropriate when redistribution effects should be included in ΔW_i, we shall generalize to the case $\alpha \neq 0$ a treatment of redistribution energy previously published.[7] Let us consider, for the moment, unit area of adsorbent surface. Then N is both the number density of adions and the total number on this area. The total system energy will then be[7] $U = (z_v e/2)\Sigma_{\text{adions}}\,\psi_i = (z_v e/2)N\psi_i$, where ψ_i includes induced polarization effects. When an adion has been removed to "infinity" and redistribution has occurred, N will become $N' \equiv N + \delta N$, where $\delta N = -1$, and ψ_i will change to $\psi_i' \equiv \psi_i + \delta\psi_i$. The new system energy (including that of the adion at "infinity") will be $U' = z_v e\psi_\infty + (z_v e/2)N'\psi_i'$, where the potential ψ_i' is calculated neglecting the small contribution from the ion at "infinity" and this neglect is compensated exactly by omitting a factor $\frac{1}{2}$, which otherwise would multiply the first term in U' involving ψ_∞. From the definitions, $W_i = \delta U \equiv U' - U$, and we may write

$$\begin{aligned} W_i &= (z_v e)\{\psi_\infty + \tfrac{1}{2}[(N+\delta N)(\psi_i + \delta\psi_i) - N\psi_i]\} \\ &\cong (z_v e)\{\psi_\infty + (\delta N/2)[\psi_i + N(\delta\psi_i/\delta N]\} \\ &\cong (z_v e)\{\psi_\infty - \tfrac{1}{2}[\psi_i + N(d\psi_i/dN)]\}, \end{aligned} \tag{5}$$

where we have neglected a term of order N^{-2}, replaced a difference quotient by a derivative, and set $\delta N = -1$ in the last expression. Since ψ_∞ approaches zero as $N \to 0$,

$$\Delta W_i = (z_v e)\{\psi_\infty - \tfrac{1}{2}[\Delta\psi_i + N(d\Delta\psi_i/dN)]\}, \tag{6}$$

an expression applying whether N denotes unit or total area. Using Eq. (6) and previous definitions, we find

$$f_3 \equiv \tfrac{1}{2}[1 + f_2 + T - (N/\psi_\infty)(d\Delta\psi_i/dN)], \tag{7}$$

which is unequal to f_2, as we shall see later, even when $\alpha \equiv 0$.

CALCULATION OF f_1^0

To establish connections with earlier work, we first consider f_1^0, no polarizability, no redistribution. Then,[7,10,13]

$$\psi_\infty^0 = 4\pi N z_v e\beta = (8\pi/\sqrt{3})(z_v e/\beta)R_1^{-2}, \tag{8}$$

where $R_1 \equiv r_1/\beta$ and the last equation applies for a regular hexagonal array. We may also write

$$R_1 = \theta^{-\frac{1}{2}} R_{1m}, \tag{9}$$

where $R_{1m} \equiv r_{1m}/\beta$ is the minimum value of R_1, that which applies when $\theta = 1$. The quantity r_{1m} will be of the order of the hard-core diameter of an adion. It may be appreciably larger than this diameter if a model such as the "immobile" system of Gadzuk and Carabateas[6] is considered for which $\theta = 1$ need not correspond to a hexagonally close packed array.

Before considering f_1^0 over the entire range of R_1, let us first investigate its limiting behavior for a mobile, hexagonal array in the limit $R_1 \to \infty$, $\theta \to 0$. The ideal dipole approximation is then appropriate and[7] $\psi_a^0 \cong \psi_{\text{dip}} = 2z_v e\sigma\beta^2/r_1^3$. The quantity $\sigma \cong 11.034$ arises

from a lattice sum.[10,13,15,16] Using the above ψ_{dip} and ψ^0_∞, we find

$$f^0{}_1=1-(\sqrt{3}\sigma/4\pi R_1)\cong 1-1.5209R_1^{-1}(R_1\to\infty), \quad (10)$$

a result which involves θ through Eq. (9). A calculation of this type was carried out by Kennedy[3]; unfortunately, he omitted a factor of β and obtained $f_{1k}{}^0\equiv 1-0.451\theta^{\frac{1}{2}}$, which can only agree with Eq. (10) for the single specific value of R_{1m}, $R_{1m}\cong 3.37$.

Since Gadzuk and Carabateas' "immobile" model is essentially equivalent to the present mobile model with $\alpha=0$ and since they calculated f on the basis of the present $f_1{}^0$, we would expect their result for this case, which holds only for the ideal dipole approximation, to agree with that of Eq. (10) when transformed from a square to hexagonal lattice. Changing a lattice sum which these authors took as 9 to its more accurate value[16] of 9.0336 and multiplying their expression for $(1-f_1{}^0)$ by $(\frac{4}{3})^{-\frac{1}{2}}$ (11.034/9.0336) to pass from a square to hexagonal lattice, we do in fact find Eq. (10).

In the opposite limit $R_1\to 0$, we expect $f_1{}^0$ to be of the form $f_1{}^0\to aR_1$. The quantity a may be evaluated exactly from our previous work[7] and is found to be

$$a\equiv(4\pi/\sqrt{3})^{-1}[(\ln 2-\gamma_1)+\ln(4\pi/\sqrt{3})] \quad (11)$$
$$\cong 0.29812.$$

Here γ_1 is the Euler constant.

An approximate expression for $f_1{}^0$ over the entire range of R_1 may be obtained using the cutoff model first introduced by Grahame.[17] Here,[7,13,18] the discrete adion and image charges are smeared and replaced by uniform sheets of charge (having the same charge density as the discrete distribution) with colinear circular vacancies each having a radius of $r_0=(\pi N)^{-\frac{1}{2}}\cong r_1/1.9046$. Let us write the connection between r_0 and r_1 more generally as $r_0\equiv pr_1$. In a treatment carried out since the first version of the present work was completed,[18] we have compared the predictions of the cutoff model using a variable p with accurate values of $\psi_a{}^0$. Such comparison leads to the result that the cutoff model can be used to calculate essentially exact potentials and fields for the fixed hexagonal array situation provided p varies over a narrow range from the Grahame value, $p_\infty\cong 0.52504$, when $z/r_1\to\infty$ to the ideal dipole value, $p_0\equiv 4\pi/\sqrt{3}\sigma$ $\cong 0.65752\cong 1/1.5209$, or less, when $z/r_1\to 0$. In the present work, as in our recent treatment of work function change on adsorption of polarizable ions,[13] we shall, for simplicity, use the constant ideal dipole value of p, $p_0\equiv 4\pi/\sqrt{3}\sigma$, since it yields more accurate results in the cutoff approximation formulas than does Grahame's value over the range of variation of z/r_1 with which we are concerned.[18]

[15] J. Topping, Proc. Roy. Soc. (London) **A114**, 67 (1927).
[16] B. M. E. van der Hoff and G. C. Benson, Can. J. Phys. **31**, 1087 (1953).
[17] D. C. Grahame, Z. Elektrochem. **62**, 264 (1958).
[18] J. R. Macdonald and C. A. Barlow, Jr., Surface Sci. (to be published).

On evaluating $f_1{}^0$ for the cutoff model using its formula[7] for $\psi_a{}^0$ with $p=p_0$, we find

$$f_{1c}{}^0=1+(2\pi R_1/\sqrt{3}\sigma)-[(2\pi R_1/\sqrt{3}\sigma)^2+1]^{\frac{1}{2}}, \quad (12)$$

which reduces properly to Eq. (10) as $R_1\to\infty$. For $R_1\to 0$, Eq. (12) yields $f_{1c}{}^0\to(2\pi/\sqrt{3}\sigma)R_1\cong 0.32876R_1$, slightly larger than the accurate value in Eq. (11). In the range $0.1\leq R_1<\infty$, the maximum deviation between the prediction of Eq. (12) and the results of the accurate non-ideal dipole treatment is less than 3.5% of $(1-f_1{}^0)$. Warner[2] and Warner and Hansen[2] have used a cutoff model to obtain an expression for $f_1{}^0$ equivalent to Eq. (12). Unfortunately, they implicitly chose the quantity $r_0/\beta\equiv pR_1$, which appears in the cutoff approximation, as $2/\sqrt{\theta}(=2R_1/R_{1m}=2r_1/r_{1m})$. This is similar to Kennedy's[3] choice and eliminates all R_{1m} dependence from $f_1{}^0$. It is equivalent to the specific selection of R_{1m} as $2/p$ and yields $R_{1m}\cong 3.04$ and 3.81 for $p=p_0$ and $p=p_\infty$, respectively. Neither value can be true in general since R_{1m} should not depend on p and may depend on the size, shape, and position of the charge centroid of adsorbed ions and on the character of the adsorbent surface.

For future calculations of f which include thermal effects, it is valuable to have a relatively simple formula which yields accurate $f_1{}^0$ values[7]. The formula from which these reference values were calculated[7] is considerably too complicated to be useful for this purpose. Equation (12) will itself be sufficiently accurate for many applications. A more accurate interpolation formula can be obtained, however, by writing

$$f_1{}^0\cong f_{1c}{}^0+F_1, \quad (13)$$

where $f_{1c}{}^0$ is given by Eq. (12) and F_1 is a rational function fitting of the difference between $f_1{}^0$ and $f_{1c}{}^0$ (see Appendix). The largest difference found between values of $f_1{}^0$ predicted by Eq. (13) and the exact values was 1.05×10^{-4} in the range of $0.01\leq R_1\leq 100$. Such accuracy is more than sufficient for all practical purposes. Note that an accurate fit for $R_1\ll 2$ is not very important; the minimum value $R_{1m}=2$ corresponds to close-packed, spherical adions with central charges, and either the shape or charge centroid location would have to be very different for R_1 to be much less than 2; alternatively, an appreciable contribution to β from the metal itself could cause $R_{1m}<2$.

As mentioned previously, the present result for $f_1{}^0$ can be converted to that appropriate for a localized model by taking $\theta=1$ in $\psi_a{}^0$ and then multiplying $(1-f_1{}^0)=\psi_a{}^0/\psi_\infty{}^0$ by θ. The resulting $f_1{}^0$ is independent of θ and equal to the mobile-model $f_1{}^0$ value at $\theta=1$.

CALCULATION OF f_1 AND f_2

Although ψ_∞ is a smeared or average potential, its value depends on discreteness-of-charge effects when $\alpha\neq 0$. As we have shown elsewhere,[13] the field $\mathcal{E}_1$ which polarizes a given adion depends on the images of this

adion and on all surrounding adions and their images. A discrete particle treatment of the situation leads to[13]

$$\psi_\infty \equiv \psi_\infty{}^0[1-g(R_1)], \tag{14}$$

where

$$g(R_1) = -(\alpha \mathcal{E}_1/z_v e\beta)$$

$$\cong \left(\frac{J}{2\epsilon_1}\right)\left\{\frac{(8\pi/\sqrt{3})R_1^{-2}}{[0.9117+(2\pi R_1/\sqrt{3}\sigma)^2]^{\frac{1}{2}}}+\tfrac{1}{2}-S\right\}, \tag{15}$$

$$\epsilon_1 \equiv 1+J\{(8\pi^3/3^{\frac{3}{2}}\sigma^2)[1+(2\pi R_1/\sqrt{3}\sigma)^2]^{-\frac{3}{2}}$$

$$-\tfrac{1}{4}+\sigma R_1^{-3}\}, \tag{16}$$

$$S \equiv 2(\beta/z_v e)(\beta \mathcal{E}_{n1}), \tag{17}$$

and

$$J \equiv \alpha/\beta^3. \tag{18}$$

In the above, the cutoff model has been used where appropriate, ϵ_1 is an effective dielectric constant, and $\mathcal{E}_{n1}$ is a "natural" polarizing field present at the surface of the adsorbent in the absence of any adsorption[10] whose effect enters via the dimensionless parameter S, defined in Eq. (17). The term in Eq. (15) involving the number $\frac{1}{2}$ arises from the field of the image of a given adion's charge, and the preceding term derives from the field at the adion coming from all surrounding non-ideal dipoles formed by other adions and their charge images. The correction term, $g(R_1)$, is zero for zero polarizability and the quantity J introduces the "feedback" upon a polarizable adion (accompanying its polarization) by the electric field arising from the image of its polarization. The $J\sigma R_1^{-3}$ term in ϵ_1 accounts for the polarizing field at a given adion arising from all surrounding coplanar ($z=\beta$) dipoles. The term $J/4$ arises from the field of the dipole image of the selected adion, and the final term comes from the ideal-dipole cutoff approximation for the field at the given adion produced by all other array image dipoles (in the plane $z=-\beta$). Although Eq. (14) has been derived for a hexagonal array, a square array of the same N should lead to essentially equal values of ψ_∞ over the range of interest of R_1.

In order to calculate f_1 we must next obtain ψ_a. When $\alpha \neq 0$, only the induced dipole image array (less the ideal dipole at the central image position) produces a potential, ψ_{ap}, which must be added to $\psi_a{}^0$ to obtain ψ_a. A sufficiently accurate approximate formula for this potential can be obtained by again using the cutoff model to represent the induced dipole image array. We require ψ_{ap} at a distance 2β in front of the center of the array with it approximated as a smeared dipole sheet having a removed circular hole of radius $r_0 = 4\pi r_1/\sqrt{3}\sigma$. A self-consistent treatment along the lines of the calculation[13] of ψ_∞ leads to

$$\psi_{ap} \equiv -(\psi_\infty{}^0/2)[1+(2\pi R_1/\sqrt{3}\sigma)^2]^{-\frac{1}{2}} g(R_1). \tag{19}$$

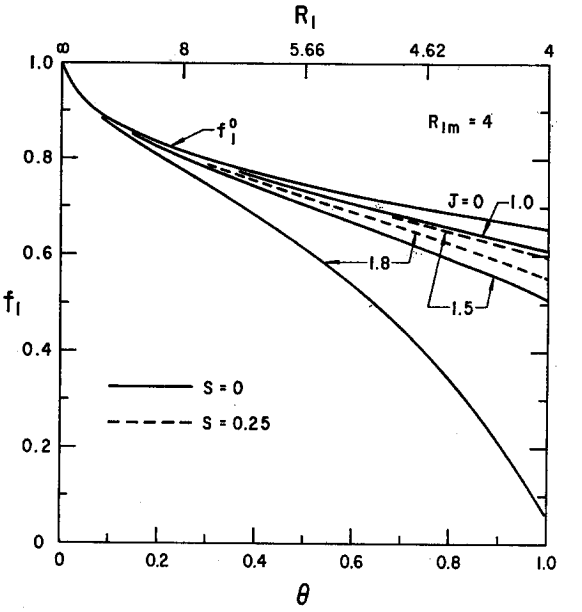

FIG. 1. The conventional penetration parameter f_1 vs θ for $R_{1m}=4$ and various values of the normalized quantities $S \equiv 2(\beta/z_v e)(\beta \mathcal{E}_{n1})$ and $J \equiv \alpha/\beta^3$ values. The dimensionless parameter $R_{1m} \equiv r_{1m}/\beta$ is the ratio of the minimum ($\theta=1$) adion nearest-neighbor distance r_{1m} to the distance β between the charge centroid of an adion and the imaging plane.

Since

$$\psi_a \equiv \psi_a{}^0 + \psi_{ap}, \tag{20}$$

$$f_1 = 1-\frac{(1-f_1{}^0)-\{[1+(2\pi R_1/\sqrt{3}\sigma)^2]^{-\frac{1}{2}} g(R_1)/2\}}{1-g(R_1)}$$

$$= \frac{f_1{}^0 - g(R_1)\{1-[1+(2\pi R_1/\sqrt{3}\sigma)^2]^{-\frac{1}{2}}/2\}}{1-g(R_1)}. \tag{21}$$

This expression reduces to $f_1{}^0$ as it should when $\alpha \to 0$.

The image dipole potential ϕ_d is just $\alpha \mathcal{E}_1/4\beta^2 = -z_v e g(R_1)/4\beta$. Thus, we may rewrite Eq. (4) as

$$T = (\sqrt{3}/64\pi)R_1{}^2[g(R_1)-g(\infty)]/[1-g(R_1)], \tag{22}$$

where

$$g(\infty) \equiv 2J(\tfrac{1}{2}-S)/(4-J). \tag{23}$$

On using Eqs. (21) and (22) in (2a), we obtain an expression for f_2.

Figures 1 and 2 show calculated values of f_1 and f_2 vs R_1 and θ for a number of J and S values. The θ scales are linear and are appropriate only for the specific choice $R_{1m}=4$, which seems to be a reasonable value for a material such as Cs^+ on tungsten.[10,13,19] The dependence of f_1 and f_2 on the upper, nonlinear R_1 scale is independent of the choice of R_{1m}.

Figure 1 shows that increasing J rapidly reduces f_1 for appreciable θ. On the other hand, $J \cong 1$ is about as

[19] J. B. Taylor and I. Langmuir, Phys. Rev. 44, 423 (1933).

large a value as one would expect to find for Cs^+ on tungsten,[13] and when $S=0$ the reduction in f_1 is relatively small. Positive values of S reduce the effect further. The value $S=0.25$ used in Fig. 1 corresponds to $\mathcal{E}_{n1}\sim 8\times 10^7$ V/cm for $z_v=1$ and $\beta=1.5$ Å. This large a value of $\mathcal{E}_{n1}$ at a distance 1.5 Å in front of the adsorbent plane is rather unlikely; although electron overlap at the surface would be expected to lead to a positive $\mathcal{E}_{n1}$, it would probably be smaller than the above. It should be noted, however, that Young[20] has found a desorption field strength for thorium on tungsten of 2.6×10^8 V/cm. For comparison, the attractive field on a point charge with $z_v=1$ arising from its image a distance $2\beta=3$ Å away is 1.6×10^8 V/cm.

Figure 1 is really included only for comparison with earlier theoretical work; as we have seen, f_2 is a better quantity for comparison with experiment than f_1. Figure 2, which has a different ordinate scale from Fig. 1, shows that positive S increases f_2 and negative S decreases it. The roles of J and S are not interchangeable, however. Here we see that for sufficiently small values of θ, increasing J increases f_2 over $f_2^0\equiv f_1^0$, while the reverse effect happens at large enough θ's. For $J\sim 1$, the effect of $\alpha\neq 0$ is appreciable, and it is made even greater by positive values of S. Thus, adion polarizability should not be neglected even when redistribution can be. We have not shown negative values of f_1 and f_2. Such values and their significance are considered later on.

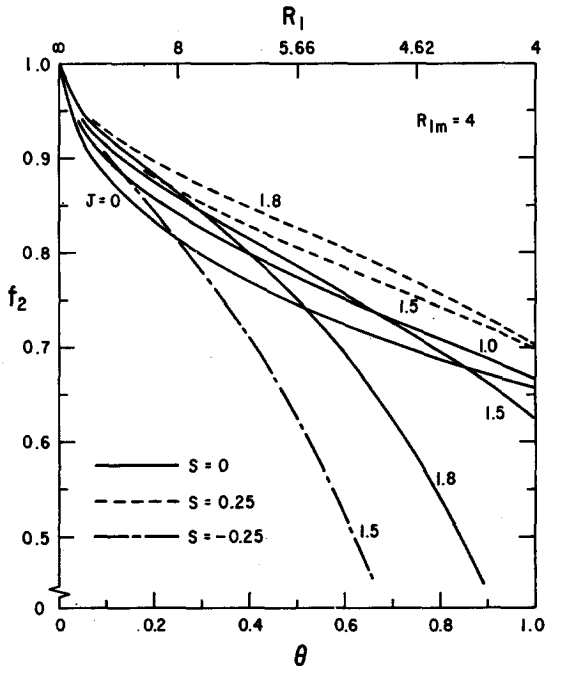

FIG. 2. The penetration parameter f_2 (with images considered but no redistribution) *vs* θ for $R_{1m}=4$ and various S and J values.

[20] R. D. Young, J. Appl. Phys. **36**, 2656 (1965).

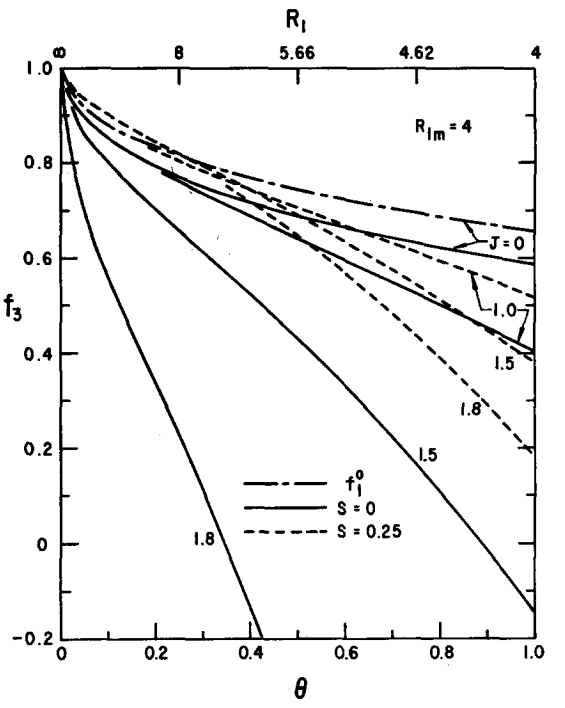

FIG. 3. The penetration parameter including images and redistribution, f_3, vs θ for $R_{1m}=4$ and various S and J values.

CALCULATION OF f_3

Equation (7) shows that to obtain f_3 we need to calculate $Nd\Delta\psi_i/dN$. We may write

$$\Delta\psi_i=\psi_a{}^0+\psi_{ap}+\phi_d-\phi_{d0}. \tag{24}$$

In the earlier work,[7] we defined and calculated

$$\begin{aligned}\eta&\equiv(N/\psi_a{}^0)(\delta\psi_a{}^0/\delta N)\\ &\cong(N/\psi_a{}^0)(d\psi_a{}^0/dN).\end{aligned} \tag{25}$$

The numerical results for η obtained there have been fitted by a rational function approximation (see Appendix); thus, this quantity is directly available for use in the calculation of f_3.

Let $\quad\zeta\equiv-(N/\psi_\infty)(d\Delta\psi_i/dN)=(R_1/2\psi_\infty)(d\Delta\psi_i/dR_1).$

Then, we may write for ζ:

$$\begin{aligned}\zeta&\cong-\eta(\psi_a{}^0/\psi_\infty)+(R_1/2\psi_\infty)[d(\psi_{ap}+\phi_d)/dR_1]\\ &\cong[1-g(R_1)]^{-1}\{\eta(f_1{}^0-1)+(R_1/2\psi_\infty{}^0)[d\psi_{ap}/dR_1]\\ &\qquad-(\sqrt{3}R_1{}^3/64\pi)[dg(R_1)/dR_1]\}.\end{aligned} \tag{26}$$

The derivatives in Eq. (26) may be calculated from the expressions already given. The substitution of the result for ζ in Eq. (7) allows f_3 to be evaluated. Such calculations have been made using a digital computer and some results are shown in Fig. 3. Because of the length of the final expression for f_3, we have not included it

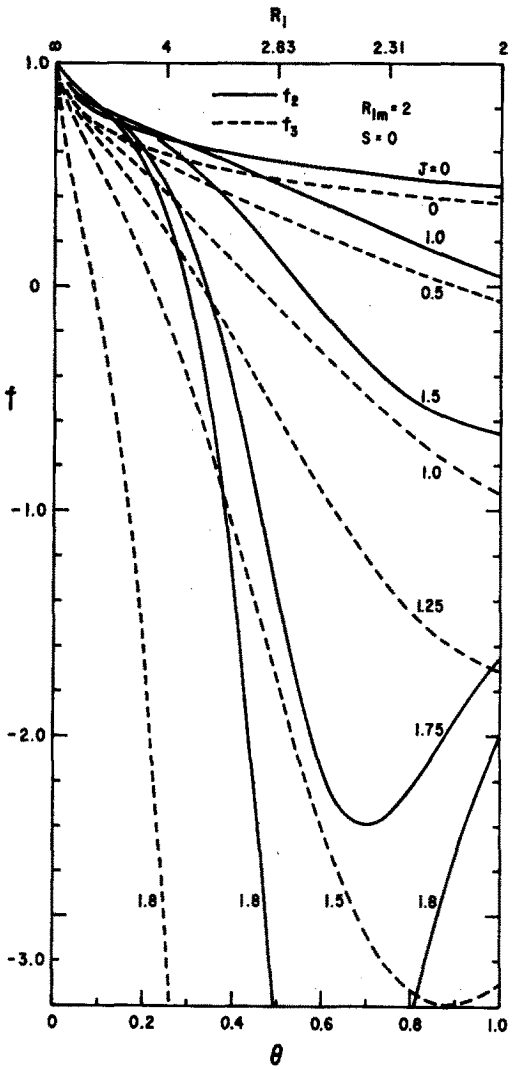

FIG. 4. The quantities f_2 and f_3 vs θ for $R_{1m}=2$, $S=0$, and various J values.

herein; the expression for f_3^0 is relatively simple, however, and is

$$f_3^0=\tfrac{1}{2}[(1+\eta)f_1^0+(1-\eta)]. \tag{27}$$

The quantity η varies from unity at $R_1=0$ to $\frac{3}{2}$ at $R_1\to\infty$.

For direct comparison, Fig. 3 shows f_1^0 as well as f_3^0 and thus indicates how much redistribution reduces f even when $\alpha\equiv 0$. For appreciable J, comparison of Figs. 2 and 3 shows that redistribution has a very pronounced lowering effect on f.

In order to show the widest range of R_1 at all likely, we have included Fig. 4, calculated for $R_{1m}=2$. Both f_2 and f_3 are plotted and only the first quarter of the θ range corresponds to that of the earlier figures. Whenever $J\gtrsim 1$, we see that f_3 is appreciably smaller algebraically than f_2 for identical J values.

Figures 3 and 4 both include negative f regions, with the negative regions being particularly pronounced for the smaller R_1 values of Fig. 4. Since previous work[13] has shown that $z_v\psi_\infty$ remains positive for $J\leq 1.85$ and $S=0$, the negative f values of Figs. 3 and 4 all imply negative ΔW_i values. For $J>1.85$, $z_v\psi_\infty$ shows a negative region and f will have one or more poles; since a J value as large as this apparently is unlikely for most situations of interest, we consider here only the range $0\leq J\leq 1.85$.

A negative value of ΔW_i implies that it requires more energy to remove an isolated adion than one in an array. Evidently, the larger the value of J, the less dense the array need be for $\Delta W_i<0$. The larger the J value, the larger the dipole induced in a given adion. These dipoles produce potential contributions which reduce both $|\psi_\infty|$ and $|\psi_a|$ but by different amounts. Thus, negative values of f_1, for example, can occur because for given J $|\psi_\infty|$ decreases more rapidly with decreasing R_1 and increasing array density than does $|\psi_a|$. This effect is the reason for possible negative values of both f_1 and f_2 and implies the surprising result that with $\alpha\neq 0$ $|\psi_a|$ can exceed $|\psi_\infty|$. This possibility is illustrated later. For f_3, negative values again arise from the above cause but redistribution energy contributions are also important. There is no redistribution for an isolated adion and redistribution of an array during removal of an adion makes it easier to remove that adion.

The quantity (f_2-f_3) is itself the redistribution energy normalized by $z_v e\psi_\infty$. It is zero at $\theta=0$ and was always positive in our calculations. For $\alpha\equiv 0$, a slight maximum occurs near $R_1=2.46$. There is none in the range $2\leq R_1\leq\infty$ for $S=0$ and $0.25\leq J\leq 1.25$ but a maximum reoccurs near $R_1=2.23$ for $J=1.5$ and has risen to $R_1\simeq 2.64$ by $J=1.8$. The larger the value of J (≤ 1.85) the larger the magnitude of (f_2-f_3).

Warner and Hansen,[2] in a company report (AI-64-20), seem to have given the only other treatment of redistribution related to the penetration parameter. The results of their treatment are not really comparable with the present ones because these authors assume no lattice structure and consider only a disordered assemblage of adions. As we have mentioned, our present treatment is inapplicable at low coverages where an ordered array is a poor approximation; Warner and Hansen's results are ouly pertinent within this range although they actually cover the range $0\leq\theta\leq 1$. Their results are still approximate even for small θ for the following reasons: First, a Bragg–Williams approximation is used in which the motions of the particles are considered independent of one another but within a potential provided by the particles themselves. Their resulting distance of nearest approach, R, is $(3/\pi^2)^{\frac{1}{2}}r_1\simeq 0.743r_1$ for a hexagonal array, or for a square array $(2/\pi)^{\frac{1}{2}}r_{1s}\simeq 0.798r_{1s}$, where r_{1s} is the nearest-neighbor distance for the square array. This choice of R, which may be identified with r_0, is also probably not a good

one: Grahame's original cutoff choice $r_0 \simeq 0.525 r_1$ also relates to a disordered array, and Levine *et al.*[21] have presented qualitative arguments that the numerical factor p should actually be less than 0.525 for a thermally disordered assemblage of adions. Further, one can readily show[22] that for the situation of a random array with no interaction between particles, the average nearest-neighbor distance is $(3/64)^{\frac{1}{2}} r_1 \simeq 0.465 r_1$. For a fixed hexagonal array, on the other hand, the numerical factor actually varies[18] from Grahame's value at $r_1 \to 0$ to $4\pi/\sqrt{3}\sigma \simeq 0.658$ for $r_1 \to \infty$. Finally, as we approach the high-temperature limit, assuming some adions still present, a regular array will have completely disappeared and the adions will move independently of one another except for steric effects which will limit their closest distance of approach in the plane to approximately twice their hard-core radii. In this limit, then, the cutoff model should be exact provided r_0 is taken as r_{1m}, a fixed value. Then $p \equiv r_0/r_1 = r_{1m}/r_1 = R_{1m}/R_1 = \sqrt{\theta}$. Although this p value could approach unity for $R_1 \sim R_{1m}$, the array would not then be disordered. The quantity R_1 will actually always be appreciably larger than R_{1m} at temperatures sufficiently high to produce considerable disorder for a given R_1, and p for a quasi-random lattice may thus be expected to be even smaller than the 0.465 value above. Note that when $p = R_{1m}/R_1$, $R_1 p = R_{1m}$ and on replacing $2\pi R_1/\sqrt{3}\sigma \equiv p_0 R_1$ by R_{1m} in Eq. (12), we find $f_{1c}{}^0 = 1 + (R_{1m}/2) - [(R_{1m}/2)^2 + 1]^{\frac{1}{2}}$ for the high-temperature limit of this quantity. When $R_{1m} = 2$, $f_{1c}{}^0 = 2 - \sqrt{2} \cong 0.586$, a result already mentioned by Warner and Hansen. From the above considerations, it appears that any choice much greater than 0.5 for a well-disordered array must be considered suspect. Certainly, 0.658 must be the upper limiting value under any condition.

In addition, Warner and Hansen have approximated the adions and their images as ideal dipoles and apparently neglected the imaging of the ideal dipoles induced in the adions. On identifying their hard-core radius r^* with β, we find that their assumptions for cesium on tungsten ($N_s = 3.56 \times 10^{14}$ cm^{-2}) lead to $\beta \cong 4.23$ Å, probably much too large. When the above value of N_s is substituted in $r_{1m} \equiv (\frac{4}{3})^{\frac{1}{2}} N_s^{-\frac{1}{2}}$, one finds $r_{1m} \cong 5.70$ Å. These values lead to $R_{1m} \cong 1.35$, a most unlikely value. It is, however, consistent with their choice of a minimum ($\theta = 1$) distance of nearest approach, $R_{\min} = r^* = \beta$. This small a nearest approach distance is, however, inconsistent with the assumption of spherical adions having their charge centroids at their centers.

Warner and Hansen have given a curve of $f(\theta)$ including redistribution and polarizability effects (with the value of α used not stated) which except at $\theta \approx 0$ lies appreciably *above* an approximate, non-ideal dipole, nonzero polarizability, cutoff curve calculated without account of redistribution. This latter curve involves the different (implicit) Warner–Hansen assumption $r_0/\beta \equiv p R_0 = 2/(\theta)^{\frac{1}{2}}$ mentioned earlier. This unjustified connection is inconsistent, as well, with their redistribution assumption since it implies $r_{0m} = 2\beta$, not β. If p is calculated from the above equation using the redistribution treatment R_{1m} value, one obtains the far too large value $p \cong 2/1.35 \cong 1.48$. Note that if Warner and Hansen had, more reasonably, defined their quantity r^* as the hard-core diameter, rather than radius, then $r^* \cong 2\beta$. It follows that $\beta \cong 2.12$ Å and $R_{1m} \cong 2.7$. Their two choices of r_{0m} would then be consistent but would still imply the unlikely value $p \cong 2/2.7 \cong 0.743$. [*Note added in proof:* Warner (private communication) states that the identification of r^* as the hard-core radius was simply an error; r^* should have been defined as $\gtrsim$ the hard-core diameter.]

Warner and Hansen ascribe the main difference between their two curves to the difference between the ideal and non-ideal dipole approximations, not to the presence of redistribution and polarizability in one calculation and their absence in another. On the basis of their work and the choices and approximations made in both calculations, this conclusion is clearly unwarranted. For our different situation treated without the above approximations, we find, in fact, that f_2 lies appreciably above f_3, not vice versa, over the whole θ range for any reasonable J value, including 0. For small θ at the limit of the applicability of the regular array model, one would expect the results of a random model which includes redistribution to join the present one without the crossover implied by Warner and Hansen's results. It appears likely that the Grahame cutoff model with redistribution will lead, when applied properly near $\theta \sim 0$, to results in agreement with these expectations.

A comparison between calculated and experimental f values is made uncertain by several factors. First, different methods of deriving f from experimental results usually give somewhat different curves.[2,4–6] The dotted and dash–dot curves of Fig. 5, for example, were both calculated using the same cesium-on-tungsten Taylor–Langmuir[19] measurements but differ in detail. Both curves have been replotted from published work by first photographically enlarging a published graph, then accurately scaling off points with a Gerber variable scale. The dotted curve is taken from the work of Gadzuk and Carabateas[6] and the dash–dot curve from that of Rasor and Warner.[5] Note that there is some uncertainty in the determination of the θ scales of these curves.

In comparing theory and experiment, we require values of β, N_s (giving r_{1m}), α, z_v, and $\mathcal{E}_{n1}$. We must also decide whether redistribution is important or not. Although it is likely that adsorbed elements are Cs^+ ions for small θ, it is probable that some adatoms are present

[21] S. Levine, J. Mingins, and G. M. Bell, Can. J. Chem. 43, 2834 (1965).

[22] C. A. Barlow, Jr., and J. R. Macdonald, *Advances in Electrochemistry and Electrochemical Engineering*, edited by P. Delahay, (to be published).

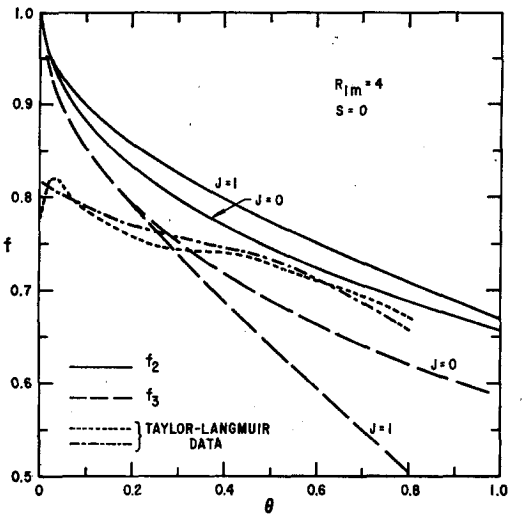

FIG. 5. Comparison of experimentally derived curves for cesium on tungsten with theoretical results for $R_{1m}=4$, $z_v=1$, $S=0$, and $J=0$ and 1.

for larger θ values.[10,13] Even if they are not present, z_v itself may possibly fall[13] with increasing θ, invalidating our assumption of a θ-independent chemical term in the total adsorption energy. Finally, no effects of a possible microscopically nonplanar imaging surface[13] have been included in the present theoretical treatment.

The appropriate value of β for Cs^+ on W is probably close to the ionic radius of Cs, ≈ 1.67 Å. The appropriate value of N_s is more uncertain. Taylor and Langmuir[19] have not fully specified their W surface. They suggest there should be one adion or adatom for each four surface tungsten atoms. Although they mention the (110) surface, for which N_s would then be 3.56×10^{14} cm^{-2}, they actually use $N_s=4.8\times10^{14}$ cm^{-2} to account for a rough surface. In fitting the Taylor–Langmuir work function data, Gyftopoulos and Levine[23] have used $N_s=4.89\times10^{14}$ cm^2. On the other hand, Warner and Hansen[2] and Rasor and Warner[5] have used 3.56×10^{14} cm^2 in their curve fitting. Finally, Gadzuk, and Carabateas[4,6] have employed assumptions equivalent to the choice $N_s\cong2.50\times10^{14}$ cm^{-2}, appropriate for a (100) surface. Recent work by Blott, Hopkins, and Lee[24] suggests that, in fact, a (100) surface does develop on a well-annealed tungsten foil. If we therefore take $N_s=2.50\times10^{14}$ cm^{-2} as the best value, then $r_{1m}\cong6.80$ Å, and $R_{1m}=4$ if $\beta=1.70$ Å. Since this is very close to the likely ionic radius, we shall employ $R_{1m}=4$ in our curve fitting.

Possible values of α for Cs^+ range[25] from about 2.3 to 3.34 Å^3. With $\beta=1.70$ Å, the maximum J is about 0.68. The quantity β would only have to be reduced to about 1.5 Å to yield $J=1$, however, if $\alpha\cong3.34$ Å^3.

[23] E. P. Gyftopoulos and J. D. Levine, J. Appl. Phys. **33**, 67 (1962).
[24] B. H. Blott, B. J. Hopkins, and T. J. Lee, Surface Sci. **3**, 491 (1965).
[25] J. Pirenne and E. Kartheuser, Physica **30**, 2005 (1964); E. Kartheuser and J. Deltour, Phys. Letters **19**, 548 (1965).

Figure 5 shows some theoretical f_2 and f_3 curves for comparison with the somewhat uncertain experimental curves shown. The values $R_{1m}=4$, $z_v=1$, $S=0$, and $J=0$ and 1 were used in calculating the f_2 and f_3 curves. We cannot expect our results to agree well with experiment for $\theta\gtrsim0.1$ because of the present neglect of thermal vibration, which becomes more significant the smaller θ. Further, because of the possible presence of adatoms and z_v dependence on θ, the adion curves probably do not apply well above $\theta\sim0.7$ or 0.8. Although the f_2 curve for $J=0$ is closest to the experimental curves in the middle range of θ, it should be remembered that a positive value of $\mathcal{E}_{n1}$ $(0<S<0.25)$ will increase f_3 values appreciably in this range (see Fig. 3), bringing them closer to the experimental curves even with $J\sim1$. Although a negative value of $\mathcal{E}_{n1}$ will reduce the f_2 values, making the $J=1$ curve closer to the experimental curves, a negative value is less likely than a positive one. With redistribution included, there appear to be one or more combinations of J (for $0<J\leq1$) and S $(0<S\leq0.25)$ which will yield quite close agreement between f_3 and the experimental curves in the middle range where the theory should apply. In view of the several uncertainties in both experimental and theoretical curves, attempts to obtain closer fitting than shown in Fig. 5 seem unwarranted.

POTENTIAL-DISTANCE DEPENDENCE

Let $\psi(Z)$ be the potential along the line perpendicular to the adsorbent through point a. Its zero is taken at the electrode, and it is defined in the absence of the central adion and its images. The quantity Z is defined as z/β. Then $\psi(1)\equiv\psi_a$ and $\psi(\infty)\equiv\psi_\infty$, where the infinities here are to be understood as the "infinity" defined earlier. A number of curves of $\psi(Z)$ for $\alpha\equiv0$ have been presented in earlier work.[7] As expected, they show a monatomic increase from zero to $\psi_\infty{}^0$. Since the results of the last sections imply that $|\psi_a|$ can actually exceed $|\psi_\infty|$ when $\alpha\neq0$, it becomes of interest to investigate the detailed shape of $\psi(Z)$ for this case. Further, this shape is of importance for electron work function measurements and calculations, since for potential shapes typical of the systems we consider, a significant fraction of the total electron current may arise from electrons which have quantum-mechanically tunnelled through a thin potential barrier region near the electrode.

We may initially divide $\psi(Z)$ into two parts:

$$\psi(Z)=\psi^0(Z)+\psi_{ap}(Z). \tag{28}$$

Although $\psi^0(Z)$ has been calculated accurately in the earlier work, we can represent it sufficiently well by the cutoff approximation to it[7] plus a rational function correction. We may thus write

$$\psi^0(Z)\cong\psi_\infty{}^0[\tfrac{1}{2}(B^+-B^-)+F_2], \tag{29}$$

where

$$B^\pm\equiv[(4\pi R_1/\sqrt{3}\sigma)^2+(Z\pm1)^2]^{\frac{1}{2}}, \tag{30}$$

and F_2 is the rational function correction (see Appendix); it is a function of both R_1 and Z.

The polarization contribution to $\psi(Z)$ may also be divided into two parts:

$$\psi_{ap}(Z)\equiv\psi_{ap1}(Z)+\psi_{ap2}(Z), \tag{31}$$

where $\psi_{ap1}(Z)$ is the potential at $\mathbf{Z}$ arising from the layer of discrete, induced dipoles in the $Z=1$ plane and $\psi_{ap2}(Z)$ arises from their images in the $Z=-1$ plane. Note that $\psi_{ap}(1)=\psi_{ap2}(1)\equiv\psi_{ap}$, since $\psi_{ap1}(1)\equiv 0$. For the $\psi_{ap}(Z)$ correction, the cutoff model approximation for each layer will be sufficiently accurate, and we find

$$\psi_{ap}(Z)=-(\psi_\infty^0/2)g(R_1)\times[(Z+1)(B^+)^{-1}+(Z-1)(B^-)^{-1}]. \tag{32}$$

When the above results are combined, we may readily calculate $\psi(Z)/\psi_\infty$. Note that in the limit $Z\to\infty$, this ratio properly goes to unity since F_2 goes to zero in the limit. For the present calculations, we require the high accuracy for $\psi^0(Z)$ given by the expression in Eq. (29) together with that in the Appendix for F_2. This is because when $[1-g(R_1)]$ is small, as it is for large J, $[\psi^0(Z)+\psi_{ap}(Z)]/\psi_\infty^0$ must approach $[1-g(R_1)]$ for appreciable Z/R_1, and we then must calculate the small difference between two relatively large numbers.

Although the present form for $\psi^0(Z)$ yields a very close approximation to accurate values of this quantity, there may be occasions where some accuracy can be sacrificed to gain simplicity. Rather than just using Eq. (29) with $F_2\equiv 0$, we have found by nonlinear least-squares fitting that added accuracy can be obtained by doing this with modified $B^\pm$ functions. In Eq. (3) let us replace $4\pi/\sqrt{3}\sigma\cong 0.65752$ by p. In the range $0\leq Z/R_1\leq 2$, least-square values of p found were 0.604, 0.620, and 0.607 for $R_1=2$, 5, and 10, respectively. Use of these values instead of $4\pi/\sqrt{3}\sigma$ reduced the standard error of the fit by about a factor of two or greater in these three cases. The largest resulting standard error, found for $R_1=5$, was about 0.0104. In the calculations reported below, we used the unmodified Eqs. (29) and (30).

Figure 6 shows calculated results for $\psi(Z)/\psi_\infty$ vs Z/R_1 for two R_1 values and a number of J values. The variable Z/R_1 is employed instead of Z because we found[7] in the $\alpha\equiv 0$ case that its use greatly reduced the dependence of curve shape on R_1.

Figure 6 indicates, as expected, that large J values can lead to $\psi(Z)>\psi_\infty$ over appreciable parts of the Z/R_1 range. In keeping with the results in earlier figures, an appreciably larger J value is required to reach a given value of $\psi(Z)$ $(>\psi_\infty)$ for R_1 of 5 than for $R_1=2$. Although these curves show increasingly high peaks, the normalized quantity $\psi(Z)/\psi_\infty^0$ *decreases* as J increases. Thus, for example, for $z_v=1$, $\beta=2$ Å, and $R_1=2$, $\psi_\infty^0\cong 26.12$ V and $\psi(1)\equiv\psi_a\simeq 6.1$, 4.8, and 4.3 V for $J=1$, 1.5, and 1.75, respectively. Similar behavior is found for $R_1=5$, but here $\psi_\infty^0\cong 4.179$ V and $\psi(4)\simeq 0.6$, 0.4, and 0.24 V for $J=1.75$, 1.90, and 1.93, respectively. Thus, the larger R_1 the larger the value of J needed for a potential barrier (or well) to appear and the broader and the smaller will the barrier be.

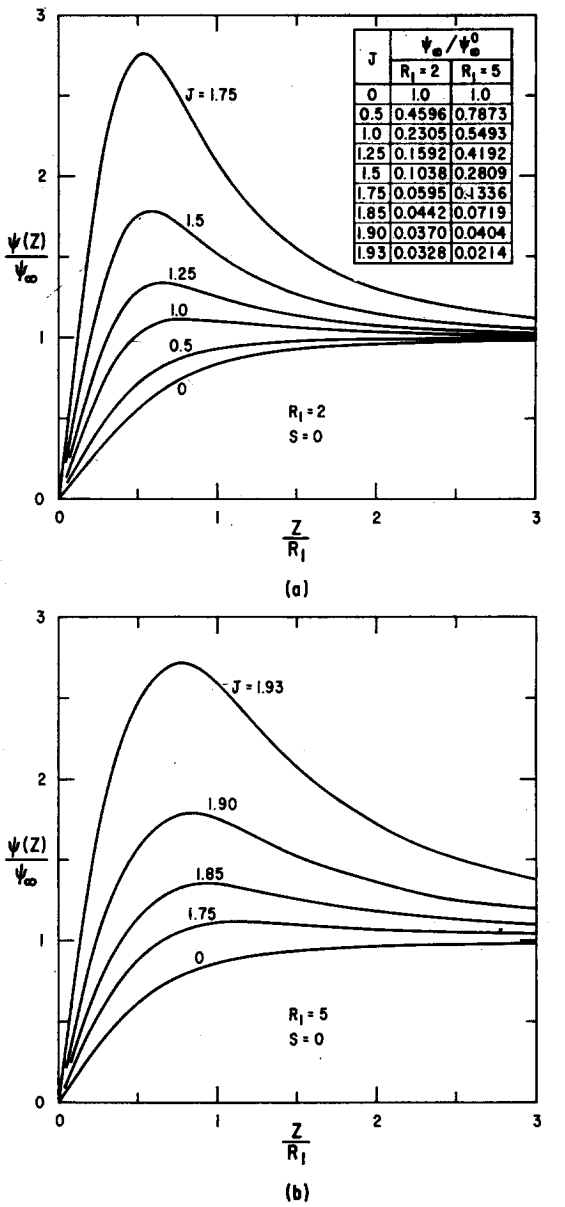

FIG. 6. Normalized potential vs normalized distance from the electrode for various J values, $S=0$, and (a) $R_1=2$, (b) $R_1=5$.

The table in Fig. 6(a) shows that for $R_1=2$ and $J=1.75$, $\psi_\infty\cong 0.06\psi_\infty^0\cong 1.55$ V using the value of ψ_∞^0 given above for $R_1=2$. In earlier work,[7] we took approximate account of the effect of polarizability on ψ_∞^0 by dividing it by an effective dielectric constant to obtain ψ_∞. Even with such a dielectric constant a function of R_1, the present results show that its introduction is a poor approximation. For example, the ϵ_1 which enters $g(R_1)$ is about 3.4 for $R_1=2$ and $J=1.75$, but the above reduction of ψ_∞^0 to ψ_∞ is by a ratio of almost 17. Further, the present subtractive type of reduction of ψ_∞^0 to ψ_∞ can lead to zero or negative values of ψ_∞, unlikely effects to arise from division by a dielectric constant alone.

Brandon[26] has given an empirical power-law relation between the polarizability of an ion core and the "univalent" radius of an ion. It indicates that the larger the radius, the larger the polarizability. As a first approximation, if we use this relation in J, we find that J also increases with ion radius. On picking a large-radius ion such as Br^-, we find $J\sim 0.9$. This is not as large as the 1.75 needed to lead to the large effects of Fig. 5, but one might expect some ions to fail to satisfy the above relation and perhaps lead to $J>1$. The present treatment holds, of course, for any constant value of z_v; when $S=0$, in fact, all normalized curves are independent of z_v.

The exact manner in which the thermionic or high-field electronic emission properties would be affected by the potential energy barriers (or wells, for $z_v>0$) we have described is uncertain in view of the varying importance of tunnelling with changes in potential shape. Quantitatively, however, we may speculate that several effects would occur: In the case of a barrier's being several volts in magnitude and 5–10 Å thick, it is unlikely that tunnelling near the vacuum level would play much of a role; therefore, the activation energy for emission would exceed the actual work function by a volt or so. Furthermore, the presence of a large "built-in" field beyond the barrier peak might possibly accelerate electrons sufficiently that space charge limiting in thermionic emission would not take place. This might be of practical importance in thermionic energy conversion systems. In the case of a deep potential well, tunnelling into the well could be a very likely process, and the sign of the field beyond the well minimum would encourage formation of a space-charge region here. It is possible that this region of trapped charge could provide a "virtual cathode" having favorable electron emission properties. More definite information concerning these effects can only be provided by an analysis of the quantum-mechanical problem of the emission process.

APPENDIX: RATIONAL FUNCTION APPROXIMATIONS

A. General Form

$$F(x)=\sum_{i=1}^{n} a_i x^i / \sum_{i=1}^{m} b_i x^i,$$

with $b_m\equiv 1$. The a_i and b_i parameters of $F(x)$ are obtained by an equi-ripple Chebyshev fitting which minimizes the absolute value of the relative difference between $F(x)$ and the function fitted for a given number of points $M\gg(n+m)$.

[26] D. G. Brandon, Surface Sci. 3, 1 (1965).

B. Improvement of $f_{1c}{}^0$

The function F_1 in Eq. (13) is given by $xF(x)$ with $x\equiv R_1$, $n=1$, $m=3$, and the values of a_i and b_i given in Table I. All numerical values are given in this appendix to eight significant figures for computer use.

TABLE I. Rational function parameters.

	F_1/R_1		χ	
i	a_i	b_i	a_i	b_i
0	−0.13373247	3.2943108	0.041685296	0.55822528
1	6.7637060×10^{-3}	2.6135061	0.046452023	−0.52515726
2	···	−0.65167653	0.13391316	1
3	···	1	0.025923739	···

C. Fitting of η

Instead of the function η defined in Eq. (25) we actually fit $\chi\equiv(\eta-1)/2$. Thus $F(x)$ is the rational function approximation to χ with $x\equiv\log R_1$, $n=3$, $m=2$, and the parameters given in Table I. This fitting was carried out for R_1 values from 1 to 100. It is not applicable for R_1 appreciably over 100; since $\eta\cong 1.499$ for $R_1=100$ and $\eta=1.5$ for $R_1=\infty$, this is not a serious limitation.

D. Fitting of $\psi^0(Z)$

The function F_2 of Eq. (29) is given by $xF(x)$ with $x\equiv Z/R_1$, $n=1$, $m=3$, and the values of a_i and b_i given in Table II for two typical R_1 values. In this table, δ_R is the maximum relative error found between the interpolation formula for $\psi^0(Z)$ and the accurate values of this quantity computed earlier.[7] The present fitting covers the range $0\leq Z/R_1\leq 3$.

TABLE II. Rational function parameters for F_2.

	$R_1=2$ $\delta_R=2.8\times10^{-4}$		$R_1=5$ $\delta_R=8.3\times10^{-4}$	
i	a_i	b_i	a_i	b_i
0	0.035197870	0.85579108	-2.5625712×10^{-4}	0.0558203367
1	5.0788303×10^{-3}	0.81188859	0.017885945	0.71840080
2	···	−1.2026512	···	−1.2040912
3	···	1	···	1